

Spectral Functions of 1D Hubbard Rings with Varying Boundary Conditions

R.N. Bannister, N. d'Ambrumenil

Department of Physics, University of Warwick, Coventry, CV4 7AL

We study the effect of varying the boundary condition on the spectral function of a finite 1D Hubbard chain, which we compute using direct (Lanczos) diagonalization of the Hamiltonian. By direct comparison with the two-body response functions and with the exact solution of the Bethe Ansatz equations, we can identify both spinon and holon features in the spectra. At half-filling the spectra have the well-known structure of a low energy holon band and its shadow—which span the whole Brillouin zone—and a spinon band present for momenta less than the Fermi momentum. New features related to the twisted boundary condition are cusps in the spinon band. We show that the spectral building principle, adapted to account for both the finite system size and the twisted boundary condition, describes the spectra well in terms of single spinon and holon excitations. We argue that these finite-size effects are a signature of spin-charge separation and that their study should help establish the existence and nature of spin-charge separation in finite-size systems.

I. INTRODUCTION

The nature of both the ground and excited states for the Hubbard model (HM) has been the theme of many recent studies. The HM itself is important not only because of its simplicity but because it is believed to include many of the principle features of strong electron correlations in a wide range of real materials. These include the 2D cuprate high- T_c materials [1] and in 1D, compounds such as TTF-TCNQ [2] and SrCuO₂ [3].

The eigenvalues can be found exactly for the 1D HM from the Bethe Ansatz (BA) equations [4]. The corresponding eigenstates can be interpreted in terms of separate populations of spin and charge excitations. The separate dynamics of spin and charge (spin-charge separation) together with other anomalous properties of the HM in 1D [5,6] are now considered to be the standard signatures of non-Fermi (or Luttinger) Liquid behavior in 1D systems and is found in other exactly soluble 1D models like the Tomonaga-Luttinger model [7,8].

The exact BA solution is not available in higher-dimensional versions of the model nor even in 1D when ‘extended’ effects such as next nearest neighbor hopping are included. Instead, one has to resort to finite-size system calculations and approximate methods. One of the problems with finite-size system calculations is that the restriction to small systems can make information about the nature of low-energy excitations in the thermodynamic limit hard to extract. Even so exact diagonalizations are an increasingly important method for studying strongly correlated electron systems [9].

Here we investigate how finite-size effects directly reflect the nature of the underlying excitations. In particular we look at how spin-charge separation manifests itself in the variation of the spectral function as a function of the boundary condition. We work with the 1D HM

where the characterization of results of direct numerical diagonalization (in terms of spinons and holons) can be independently verified by comparing with the exact BA solution.

There has already been considerable interest in how the HM behaves as the boundary conditions are changed by introducing a phase twist, δ , in the periodic boundary conditions (PBC), *ie* $c_{i+N}^\dagger = e^{-i\delta} c_i^\dagger$. This corresponds to threading the loop formed by the N sites in the chain with the magnetic flux $\Phi_0 \delta / 2\pi$, where Φ_0 is the flux quantum and the c_i^\dagger create electrons in orbitals at site i . One consequence of the phase twist is to shift all allowed momenta by an amount δ/N yielding the allowed momenta:

$$k = \frac{2n\pi + \delta}{N}, \quad (1)$$

for n integer. When an electron is added or removed, the many body system changes its total momentum by an amount corresponding to one of the allowed values in (1). By varying δ we can, in effect, simulate a continuously varying momentum in a finite system.

The ground state energy of the 1D HM has an interesting structure when plotted as a function of δ [11–13]. For large U , there are oscillations in the ground state energy which are often found to vary with more than one period. These oscillations—which may include periodicities of 1, $1/N_e$ and N_\downarrow/N_e (for a total of N_e electrons present, N_\downarrow of them being spin-down)—give rise to cusps in the energy variation for a finite system. These effects are accounted for in terms of transitions mainly in the sea of spin particles as δ is changed [11,12]. The ground state energy is found to be consistent with a hole in the spin sea which traverses from one Fermi point to the other as the boundary condition is varied. (Since the spin ‘excitations’ have zero energy, the spin sector can be used by

the system as a momentum bank charging no ‘interest’.)

To gain a quantitative picture of excitations in the 1D HM, various authors have used different approximations and direct diagonalizations. By using Lanczos diagonalization, Kim and collaborators [3,14] calculated the photoemission spectral function, $A(k, \omega)$, for a finite half-filled system with fixed PBC (they actually considered the t - J model). Their result, which is essentially the same as that of the strongly correlated HM, consists of spectral weight belonging to two bands, which they identified with separated spin and charge degrees of freedom. The ‘charge band’ (of width $4|t|$ and present in the whole Brillouin zone) traces out the dispersion of the so-called holon excitations. The ‘spin band’ (of width $\pi J/2$ for $J = 4t^2/U$) exists only for $|k| < k_F$ ($k_F = \pi/2$) and is associated with an excitation of the corresponding spinon population. This structure of the spectral function is a natural consequence of spin-charge separation and can be explained through a semi-intuitive picture which has been termed the ‘spectral building principle’ (SBP) [15,3] (see section IV below).

In this paper we study the spectral functions of small 1D systems ($N = 12$) at half-filling and in the presence of variable twisted PBC’s. We show how the spectral building principle can be adapted to account for the features that appear in the spinon bands and suggest that these features provide a natural test in finite system calculations for spin-charge separation. The structure of this paper is as follows: In section II we outline the procedure which we adopt to calculate and analyze the spectral functions of the 1D HM with twisted PBC. Our results are shown in section III. In section IV we review and adapt the SBP to help interpret our spectra. Finally in section V we summarize our findings and speculate how the SBP could have a bearing on systems other than the half-filled HM in 1D.

II. PROCEDURE

We compute the spectral functions using the method used by Tohyama and Maekawa [16]. For a given δ we compute the spectral function $A(k, \omega)$,

$$A(k, \omega) = \frac{1}{N} \sum_m |\langle \psi_m^{N_e-1} | c_{k\downarrow} | \psi_0^{N_e} \rangle|^2 \delta(\omega + [E_m^{N_e-1} - E_0^{N_e}]) \quad (2)$$

at those momenta consistent with the choice of δ . We use the standard Lanczos recursion method [17]. In eq. (2), $|\psi_m^{N_e}\rangle$ is the m th energy eigenvector (with energy $E_m^{N_e}$) of the N_e -electron system (at half-filling there are equal populations of each spin species). All wavefunctions and energies are dependent upon δ . Following [16] we analyze the peaks in the spectral function by computing the

complementary (fixed particle number) dynamic spin and charge correlation functions defined respectively as,

$$S(q, \omega) = \frac{1}{N} \sum_m |\langle \psi_m^{N_e-1} | S(q) | \psi_0^{N_e-1} \rangle|^2 \times \delta(\omega + [E_m^{N_e-1} - E_0^{N_e-1}]), \quad (3)$$

$$N(q, \omega) = \frac{1}{N} \sum_m |\langle \psi_m^{N_e-1} | N(q) | \psi_0^{N_e-1} \rangle|^2 \times \delta(\omega + [E_m^{N_e-1} - E_0^{N_e-1}]). \quad (4)$$

The spin and charge operators, $S(q)$ and $N(q)$ are

$$S(q) = \sum_i \exp(iqr_i)(n_{i\uparrow} - n_{i\downarrow} - S_0) \quad (5)$$

$$N(q) = \sum_i \exp(iqr_i)(n_{i\uparrow} + n_{i\downarrow} - N_0) \quad (6)$$

where the summations are over sites, S_0 and N_0 are the spin and charge backgrounds ($S_0 = (N_\uparrow - N_\downarrow)/N$ and $N_0 = (N_\uparrow + N_\downarrow)/N$) and $n_{i\sigma} = c_{i\sigma}^\dagger c_{i\sigma}$.

The momentum transfer, q , is defined via $q = k_F - k$. The Fermi momentum, k_F is defined as the momentum state with the highest single electron energy which is occupied at half-filling in the non-interacting ($U = 0$) case and which has positive momentum. The restriction to $k_F > 0$ is important in order to maintain the association of excitations around the positive Fermi point with small q . Consequently, for some choices of δ , $|\psi_0^{N_e-1}\rangle$ in (3) and (4) is not the true ground state, but is the lowest energy level in the subspace of states which share the same momentum as $c_{k_F\downarrow}|\psi_0^{N_e}\rangle$. Since both k and k_F depend upon δ according to eq. (1), the effect of δ cancels in q as expected (q is a momentum transfer and the spacing between the allowed wavenumbers k is fixed).

The dynamic spin and charge correlation functions probe the properties of the excitations in the $N_e - 1$ electron system. A level with a strong response in $S(q, \omega)$ is taken to indicate a spinon excitation. Features in $N(q, \omega)$ are then associated with holon excitations. Some levels could be due to multiple excitations in one or both sets of particles. By comparing the spectral function to the corresponding spectra of $S(q, \omega)$ and $N(q, \omega)$ we have been able to classify many spectral features by identifying which excitations are spinon-like and which are holon-like. This procedure is repeated over the range of δ -values ($0 \leq \delta \leq 2\pi$). This allows us to plot spectra as a function of a quasi-continuous momentum variable, although strictly such spectra are taken from an ensemble of systems with differing boundary conditions.

Because the HM is integrable in 1D, we can independently verify our assignments of the features we find in the spectral function by reference to solutions to the BA equations. For an N -site Hubbard chain with N_e particles and N_\downarrow down spins and a twisted boundary condition these are ($t = 1$)

$$k_j N = 2\pi I_j + \delta - \sum_{\alpha=1}^{N_e} 2 \tan^{-1} \left[\frac{4(\sin k_i - \lambda_\alpha)}{U} \right] \quad (7)$$

and

$$-\sum_{i=1}^{N_e} 2 \tan^{-1} \left[\frac{4(\sin k_i - \lambda_\alpha)}{U} \right] = 2\pi J_\alpha + \sum_{\alpha=1}^{N_\downarrow} \tan^{-1} \left[\frac{2(\lambda_\alpha - \lambda_\beta)}{U} \right]. \quad (8)$$

The quantum numbers I_j, J_α characterize the charge and spin degrees of freedom. They are either integer or half-odd integer according to the conditions

$$I_j = \frac{N_\downarrow}{2} (\text{mod}1) \quad (9)$$

$$J_\alpha = \frac{N_e - N_\downarrow + 1}{2} (\text{mod}1). \quad (10)$$

The total energy E and total momentum P of the system of particles is

$$E = -2 \sum_{j=1}^{N_e} \cos k_j \quad (11)$$

$$P = \sum_{j=1}^{N_e} k_j = \frac{2\pi}{N} \left[\sum_{j=1}^{N_e} I_j + \sum_{\alpha=1}^{N_\downarrow} J_\alpha \right] - \delta \frac{N_e}{N}. \quad (12)$$

The BA equations (7) and (8) are easy to solve numerically assuming real rapidities k_j, λ_α by simple root searching.

III. RESULTS

Figure 1 is the spectral function for the half-filled 12-site Hubbard band with $U = 10$ and antiperiodic ($\delta = \pi$) boundary conditions computed using direct diagonalization (Lanczos). The curves are cross sections through the spectrum at those momenta consistent with this choice of δ . The peaks have been Lorentzian broadened as a guide to the eye. In order to label the peaks (spin or charge-like), spectra of the spin and charge correlation functions have been superimposed and the dispersive tendencies of the main spin and charge-like peaks have been drawn in thin lines. The results are very similar to those of Kim et al. [14]

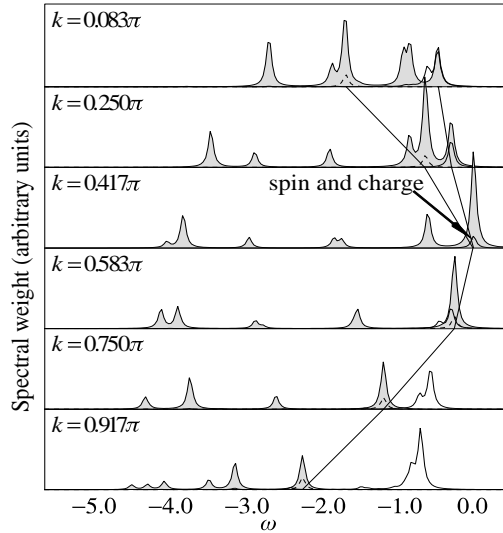


FIG. 1. The raw spectral functions computed using Lanczos for a ring of 12 sites at half-filling with $U = 10$ and $\delta = \pi$. The spectral functions (shaded) are shown together with the diagnostic spin (continuous line) and charge (broken line) correlation functions for the 11 electron system. The peaks have been Lorentzian broadened to $\Delta\omega = 0.04|t|$ and the correlation functions have been scaled by a factor 5. Some peaks have been joined between different k values with thin lines to illustrate the dispersive nature of the principle excitations.

To illustrate the essential features of the spectra obtained by exact numerical diagonalization as δ is varied, we show the spectra in the k - ω plane. Each peak in the spectral function $A(k, \omega)$ is represented by a symbol centered about its momentum (k) and energy (ω). Figure 2a is for the same system as in Figure 1 but for a range of δ . The size of the symbols is used to denote the spectral weight while (as indicated in the inset to Figure 2a) the shape is used to distinguish between spin and charge excitations. For some peaks denoted by shaded squares, there is a contribution from both types of correlation (as indicated for example in Figure 1 at $k = 0.417\pi$). The remaining peaks which cannot be identified through the correlation functions are denoted by crosses. We also show the spin and charge correlation functions for this system (Figures 2b and 2c respectively) which were used to classify the features in the spectral function into ‘charge-like’ and ‘spin-like’. (To make the comparison with $A(k, \omega)$, straightforward $S(q = k_F - k, \omega)$ and $N(q = k_F - k, \omega)$ are shown as functions of k .)

The vertical lines on Figure 2 denote those momenta corresponding to the choice of δ in (1) which give rise to a closed-shell configuration for the electrons in the ground state. For the 12 particle system this corresponds to $\delta = \pi$. The separation between two adjacent vertical lines corresponds to a change of 2π in δ .

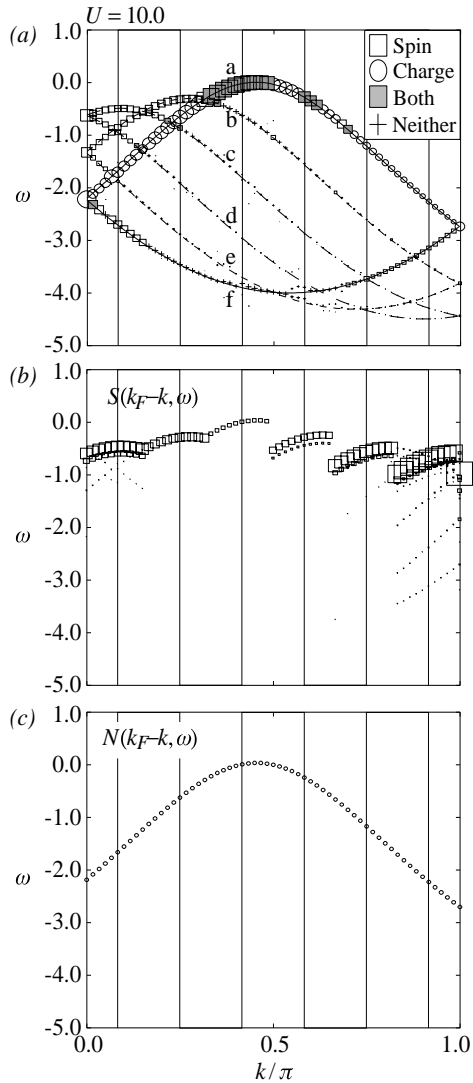


FIG. 2. (a) The spectral function for the 12-site half-filled system with $U = 10$ computed by varying the boundary condition parameter δ . Peaks in the spectral function are classified into ‘spin-like’, ‘charge-like’, ‘both’ and ‘neither’ using the spin and charge correlation functions for the 11 particle system shown in (b) and (c). The areas of the symbols is proportional to the spectral weight in (a) and to the amplitude of the correlation functions in (b) and (c). The continuous curves in 2(a) are those obtained from solving the BA equations and the labeling a-f denotes the quantum numbers J_α shown in Table I.

In Figure 2, the solutions of the BA equations are superimposed on the results obtained by direct diagonalization. Each curve, labeled by the letters a-f, corresponds to a different choice of quantum numbers J_α as shown in Table I. The I_J distribution in each case is that of a single holon, the position of which traces out the complete holon band as the phase shift is varied. The agreement between the labeling of the results of the direct diagonalization and the results of the BA calculation show that

the numerical procedure based on comparison with spin and charge correlation is a very reliable way of identifying the nature of the excitations involved.

In Figure 2a there are obvious features related to the twisted PBC. At low binding energies and low momenta (upper left part of Figure 2a), there is a series of ‘humps’ in the spin-like band, which have an approximate symmetry about the closed shell lines. The main charge-like band, which exists over the full Brillouin zone (band ‘a’ in Figure 2a), has the same shape as one would expect to recover in the thermodynamic limit. As we argue in section IV, these effects of the twisted PBC should be expected and are typical for systems with spin-charge separation.

The extension of the charge band to negative momenta (not shown) and then reflected about $k = 0$ gives the feature which disperses with positive curvature in the high energy region of Figure 2a (band ‘f’). Something similar to this curve was seen by Penc et al. [18] where it was interpreted as a shadow of the main holon band shifted in momentum by $2k_F$ (we will refer to this band as the ‘shadow band’). Penc et al suggest that this shift is due to scattering by spin fluctuations at $2k_F$ (the spin correlation function has a singularity at $2k_F$ for strongly correlated electrons [10]). Most of the shadow band is of undefined nature in our results (although some peaks do have a very weak spin correlation). The explanation of this feature in the context of the Spectral Building Principle (section IV) is compatible with that of Penc et al.

There are some features in the photoemission spectrum which our comparison with the two-particle correlation function does not clearly identify as being related to either spin or charge correlations. These tend to have low spectral weight and/or to be at energies far from the Fermi energy. There are conversely also features in the correlation functions which are not relevant to photoemission. The spin correlation function for example exhibits very strong peaks at $k > k_F$ (Figure 2b). These have no photoemission association except where they cross the charge band. We attribute these humps in the correlation function for $k > k_F$ to multiple holon and spinon excitations (section IV).

| | J_α | | | | | |
|---|------------|------|------|-----|-----|-----|
| a | -2.5 | -1.5 | -0.5 | 0.5 | 1.5 | X |
| b | -2.5 | -1.5 | -0.5 | 0.5 | X | 2.5 |
| c | -2.5 | -1.5 | -0.5 | X | 1.5 | 2.5 |
| d | -2.5 | -1.5 | X | 0.5 | 1.5 | 2.5 |
| e | -2.5 | X | -0.5 | 0.5 | 1.5 | 2.5 |
| f | X | -1.5 | -0.5 | 0.5 | 1.5 | 2.5 |

TABLE I. The spin quantum numbers for the various solutions (labeled a-f in Figures 2 and 3) to the Bethe Ansatz equations (8). The hole in the spinon band or ‘antispinon’ is denoted by X.

The new spinon related structure in the spectral function is a finite-size effect. There are $N/2 - 1$ spinon cusps present for $-\pi \leq k < \pi$. For this system and all systems with $N/2$ even, there is a cusp at $k = 0$, while for odd $N/2$ the cusp is displaced from $k = 0$ by π/N . The range just below k_F in which the spectral function has mixed spin and charge character is of width π/N and becomes a single point in the thermodynamic limit.

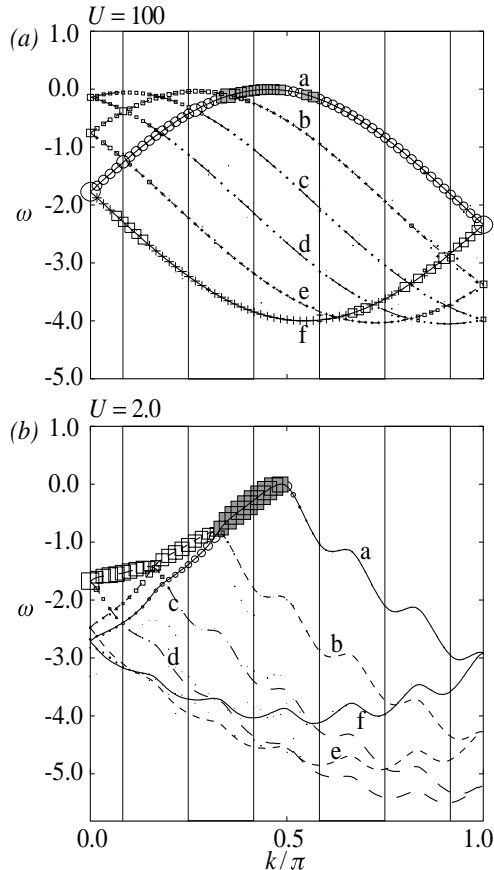


FIG. 3. As Figure 2a but for $U = 100$ and $U = 2$.

Results for $U = 100$ are shown in Figure 3a. The basic spectral structure of Figures 2a and 3a is similar. There is more spectral weight in the high energy regions than for $U = 10$ with the shadow band having almost the same weight as the main holon band. The spinon band width parameter $J \sim 4t^2/U$ tends to zero in this limit and, in the infinite system, the spinon excitations for $U \rightarrow \infty$ do not disperse [19]. Unlike the spinon bandwidth, the humps in the spinon part of the spectra do not scale with $1/U$.

In the weakly correlated case of $U = 2$ shown in Figure 3b, the main holon band for $k > k_F$ and the shadow band have a decreasing share of the spectral weight. (As the interaction is reduced, the spectrum is tending towards a conventional quasiparticle band with an electron Fermi surface.) There is still a two peak structure for $k < k_F$,

although the identification of spin and charge-like character of the peaks in Figure 3b is only an indication of which excitation-type dominates, as there is notable mixing of spin and charge correlations. This is seen in both the charge and spin correlation functions which show a response at the corresponding frequencies. The humps in the weak holon band for $k > k_F$ develop into the one-particle two-hole excitations of the non-interacting case (where of course they have no spectral weight).

IV. THE SPECTRAL BUILDING PRINCIPLE (SBP)

The photoemission spectrum for a strongly correlated HM in the thermodynamic limit can be explained using the semi-phenomenological SBP [15,3]. The SBP determines where spectral weight is expected and classifies the features as spin or charge-like. The SBP does not predict the magnitude of the spectral weight itself and this information must be found by other means like exact diagonalization or approximate methods.

The SBP assumes that the ground state of the half-filled system is made up of a half-filled spinon band containing N_\downarrow spinons and an empty holon band, with energies $E_s(k_s)$ and $E_h(k_h)$ and momenta k_s and k_h for the spinon and holon respectively. The SBP treats the spinons and holons as independent excitations obeying the Pauli exclusion principle. At half-filling the dispersion relations are given by [20],

$$E_s(k_s) = \frac{\pi}{2} J \cos(k_s) \quad (13)$$

$$E_h(k_h) = 2|t| \cos(k_h). \quad (14)$$

The peaks on the spectral function are assumed to involve a single anti-spinon excitation (the annihilation of a spinon from the spinon sea) and a single holon excitation (the creation of a holon in the empty holon dispersion curve). Taking the spinons and holons to be independent excitations, the electron Green's function would then be expected to be well-described by a convolution of the spinon and holon Green's functions. Conservation of energy and momentum would imply

$$\omega = E_s - E_h \quad (15)$$

$$k = k_s - k_h. \quad (16)$$

Here ω and k , as in Figures 2a and 3, are the energy and momentum lost by the system when an electron is photoemitted.

According to the SBP, a peak on the spinon band in the spectral function in the strongly correlated limit is interpreted as a specific anti-spinon excitation in combination with the (fixed) lowest energy holon excitation at k_h^0 . In the thermodynamic limit, $k_h^0 = \pi$. By varying the choice of anti-spinon excitation and using (13)-(16), this gives

the entire spinon band, $\omega_s(k) = (\pi J/2) \cos(k + \pi) + 2|t|$ but with a cut-off at the spinon Fermi surface at $k = \pm\pi/2$. In the photoemission spectrum, the occupied regions of the spinon dispersion have been shifted in energy and momentum by the holon excitation at k_h^0 . Likewise, the SBP assumes that holon bands (main and shadow) are made up of all possible holon excitations together with a fixed anti-spinon excitation of lowest energy at $k_s^0 = \pm\pi/2$, corresponding to spinon annihilation at the spinon Fermi points. The holon bands in the spectral function have the form, $\omega_h(k) = -2|t| \cos(k \mp \pi/2)$. Since the holon bands measure the unoccupied regions of the holon dispersion, the holon band observed in the photoemission spectrum extends throughout the Brillouin zone.

The SBP as outlined in [15,3] describes the spectra in the thermodynamic limit. In order to proceed to finite systems and, in particular, to explain the effect of the twisted PBC we need to determine how the spinons and holons should respond to δ . We assume that the holon and spinon momenta are given by

$$k_{hj} = \frac{2\pi I_j + \delta}{N} \quad (17)$$

$$k_{s\alpha} = \frac{2\pi J_\alpha}{N} \quad (18)$$

with the I_j and J_α integer or half-integer as in (9) and (10). These quantities were introduced previously in [8] to help elucidate the connection between the exact eigenstates of the Hubbard model and the exact solution of the Tomonaga-Luttinger liquid. We have generalized them by including the phase shift term in (17).

The allowed values for the holon quantum numbers k_h, k_s or (equivalently) I_j, J_α are functions of the number of particles N_e and the spin polarization N_\downarrow . The photoemission process measures the energy of the $N_e - 1$ particle system as a function of the missing energy and momenta, so it is natural to expect the quantum numbers of the $N_e - 1$ particle system to characterize this missing energy and momentum. We therefore assume that the parity conditions on I_j and J_α are those for the the $N_e - 1$ particle system.

When we compute the spectral function using Lanczos and the energy dispersion by directly solving the BA equations, we measure frequency with respect to the ground state of the system for the same boundary condition. This energy itself depends on δ and this effect is not accounted for by the SBP when we assume the relation (15). For $U = 2$, the variation in the ground state energy of the half-filled case is less than 10% of the spinon bandwidth and is smaller for larger U . For the spectral function taken for systems which are not half-filled and with no gap the picture is more complicated and will be addressed in a later publication.

Figure 4 shows the positions of the spinon and holon peaks computed using the SBP for the case $U = 100$ and

should be compared with the numerical results of Figure 3a. The spinon regions are denoted by squares and the holons with circles. The agreement is good bearing in mind that only the spectral features which are associated with k_h^0 and k_s^0 are reproduced in Figure 4). The main holon band, the shadow band and the spinon cusps are reproduced. The number of cusps and their positions agree well with the numerical result and this picture also gives an offset of the top-most energy of the holon band to a slightly lower momentum than k_F which is evident in the numerical result too. Shown for comparison is the result for the thermodynamic limit where there are no cusps and the top of the holon band is at k_F exactly.

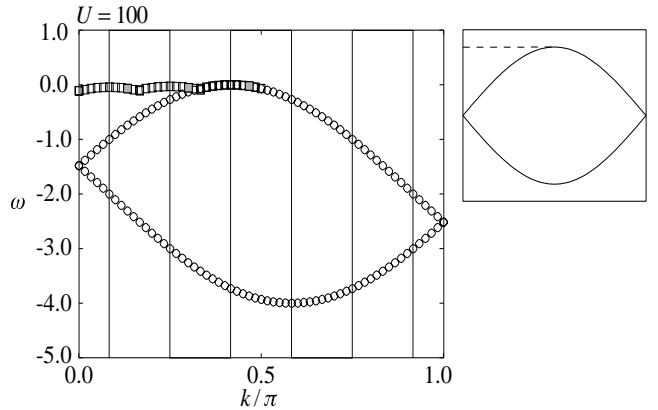


FIG. 4. The main picture (left) shows the photoemission spectrum for $N = 12$, $N_e = 12$, $N_\downarrow = 6$ and $U = 100$ computed on the basis of the SBP (squares=spinon, circles=holon) and should be compared with the result of Figure 3a. The shaded points are for reference in the text to follow. The small plot shows the corresponding result in the thermodynamic limit (continuous line=charge, broken line=spin).

The shape of the spectra Figure 4 can be understood by considering the holon and spinon dispersions for a given δ shown in Figure 5. For the spinon band in Figure 4 the set of occupied states of the spinon dispersion are all shifted together by the lowest energy holon excitation—labeled ‘A’ in Figure 5 (note that the spinon bandwidth is exaggerated in Figure 5). According to (13) and (14) this gives one set of equally spaced points on the spinon band in Figure 4 (the shaded points). Varying δ changes both the energy and momentum of the lowest energy holon while the spinon energy is (by assumption) independent of δ . As a result, each peak in the spinon band of the spectral function is shifted to a slightly different position. The humps observed in the spinon band of the spectral function then simply reflect the variation with δ of the holon state labeled by ‘A’. At certain values of δ the lowest energy holon excitation changes its momentum discontinuously as the state previously labeled by ‘A’ moves up the holon band. Whenever this occurs it gives rise to the cusps in the spinon band in the spectral function.

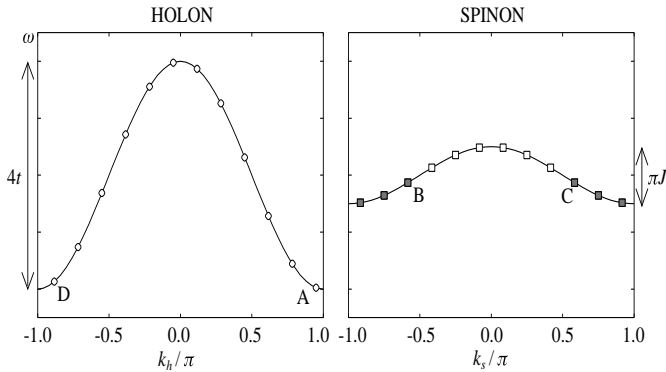


FIG. 5. The holon and spinon dispersions for the finite system $N = 12$, $N_e = 12$, $N_\downarrow = 6$ and $\delta = 1.6\pi$. Open (filled) symbols denote unoccupied (occupied) holon and spinon states. The allowed holon states change with δ but those of the spinon are static.

The form of holon bands in the spectral function can also be understood using the SBP. The shift of the holon dispersion by the spinon excitation ‘B’ gives rise to the main holon band (the upper holon band in Figure 4). Since (by assumption) the allowed momenta in the spinon dispersion are independent of δ , the holon dispersion is shifted by a constant amount as δ is varied. This is the reason why the holon bands in the numerical spectra are smooth and free of cusps in the strongly correlated limit. The alternative spinon excitation, ‘C’, has the same energy as ‘B’ but shifts the holon dispersion by a different momentum. This leads to the so-called shadow band in the spectral function (lower holon band in Figure 4). The momentum difference between ‘B’ and ‘C’ is $2k_F$ (true for all fillings) which explains why the shadow band is displaced by $2k_F$ from the main holon band.

The coupling between spin and charge which exists for moderate U means that assuming completely independent spinon and holon bands as in (13) and (14) is no longer strictly valid. Even so it is still possible to explain the spectra using the SBP, although the non-zero spinon bandwidth J introduces a minor complication as we explain below.

If we implement the SBP exactly as described above for the large U case, the low energy peaks predicted by the SBP do not agree completely with what we find using direct diagonalization and the BA solution. Figure 6a shows the photoemission spectrum computed on the basis of the SBP for $U = 10$ ($J = 0.4$) and $N = 12$ at half-filling (shown in the inset is the $N \rightarrow \infty$ result for comparison). Unlike the numerical result of Figure 2a there appear to be discontinuities in the spinon band while the holon bands look very similar to what we found numerically (see Figure 2a). These discontinuities come about because we have assumed that, as in the large U case, the spinon band of the photoemission spectrum corresponds to the combination of a spinon with the *lowest* energy holon excitations as before. Whereas this is cor-

rect for most momenta (with $k \leq \pi/2$) in Figure 6a, it is not true for the range of momenta highlighted by the horizontal ‘bars’ in the top-left of Figure 6a. We find that for these electron momenta, lower energy electronic states can be formed by combining a spinon excitation with the slightly *higher* energy holon excitations at point ‘D’ in Figure 5. Figure 6b shows the photoemission spectrum computed using the SBP adjusted to allow also for low energy spinon and holon combinations (*ie* using states at ‘D’ as well as ‘A’ in Figure 5). Although it might seem peculiar that an electronic state formed from a higher energy holon state (‘D’) can be responsible for lower energy electronic states, it can be explained as follows. The holon at point ‘D’ in Figure 5 (k_h^D, E_h^D) has a higher momentum than ‘A’ (k_h^A, E_h^A) (after adding 2π to k_h^D). To form a hole with given momentum, the spinon state combined with the holon state at ‘D’ will be at a different point on the spinon band. The cost in energy of using the more energetic holon state ‘D’ can then be compensated by a lower spinon energy. This adjustment is not necessary for the $U \rightarrow \infty$ case since there the spinon band is flat.

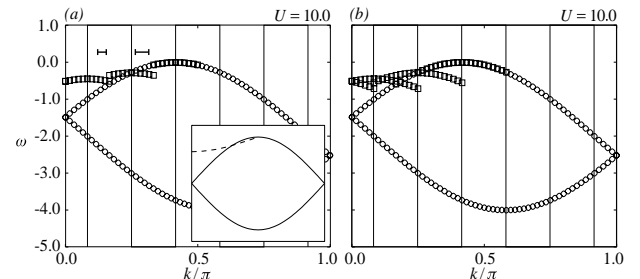


FIG. 6. Spectral function computed using the spectral building principle for $N = 12$, $N_e = 12$, $N_\downarrow = 6$ and $U = 10$. In (a) the spinon (holon) band is shifted by the very lowest energy holon (anti-spinon) excitations only. The inset is for the thermodynamic limit (continuous line = charge, broken line = spin). In (b) we allow the spinon dispersion to be shifted by the next lowest energy holon excitations also. This should be compared with Figure 2a.

Although $U = 2$ does not represent a weakly correlated system, it is too small for the SBP to work well. We find, in fact, that the SBP ceases to work well below $U \approx 4$, where the holon band starts to develop humps as a function of δ . We have tracked these humps in the exact BA solution as a function of U down to small U ($U < 0.1$). They develop into the two-hole and one-particle excitations of the non-interacting system, where of course they have vanishing spectral weight.

In the SBP plots (Figures 4 and 6), we have shown only those peaks which are firmly classified using the results of the spin and charge correlation functions. These turn out to those associated with the lowest (or in some

cases low-lying) spinon or holon excitations. The numerical spectra contain many other peaks in addition to the spinon and holon bands. By taking every possible combination of *single* holon and anti-spinon excitations - regardless of energy - the SBP can reproduce essentially all the peaks in the spectral function. It is clear then that the spectral function are dominated by the creation of *single* holon plus anti-spinon excitations.

Other classes of excitation exist which can be accounted for using the SBP but which are invisible in the spectral function. For example for the $U = 10$ system of Figure 2 it is clear that that there are contributions to the spin correlation function for $k > k_F$ for momenta $k > \pi/2$ (there is no significant charge correlation in addition to that already discussed). We attribute these ‘extra’ humps to multiple excitations, namely the holon and anti-spinon excitations already described accompanied by a spinon/anti-spinon pair (a spin wave). The effect of the twisted PBC makes these easy to identify, as the spinon humps at $k > k_F$ appear as images of one or more of the original humps in the spinon band but shifted by the extra momentum and energy of the spinon/anti-spinon pair. The spin waves can provide potentially any momentum in the set $\{2n\pi/N\}$ and an energy which is finite but small (due to the narrow width of the spinon band).

V. SUMMARY

We have studied the photoemission spectrum of 1D Hubbard model at half-filling as a function of the periodic boundary condition (PBC) in finite size chains. We have shown that the finite-size effects can be well explained using the spectral building principle (SBP, [3,15]) adapted to the case of finite systems and the twisted PBC, in terms of independent populations of spinons and holons. We have found that the photoemission spectral functions are explained for $U > \sim 4$ by assuming that only the holons are directly dependent on the twisted PBC and that one holon-one antispinon pairs account for essentially all the spectral weight. Other excitations involving additional spin-wave processes are observed in the spin correlation function.

The key feature found in the strongly correlated systems ($U > \sim 4$), in which the spinons and holons may be thought of as independent excitations, are the ‘humps’ in the spinon bands of the photoemission spectra. We have shown that the curvature of these humps directly reflects the curvature of the holon dispersion at the bottom of the holon band and so could be used to extract directly

the holon effective mass in cases where there is no direct independent way to compute this quantity.

We have restricted our study to the 1D nearest neighbor Hubbard model where we have been able to show that identifying the spin and charge excitation bands using the corresponding correlation functions agrees exactly with the results from Bethe Ansatz exact calculations. These results suggest that this method can be extended to other 1D systems and higher dimensional systems for which there is no exact BA solution for the model [21].

We wish to thank the EPSRC for providing the funding for this work.

- [1] P.W. Anderson and Y. Ren, *High Temperature Superconductivity Proceedings*, Los Alamos 1989 (1990).
- [2] P.F. Maldague, Phys. Rev. B **16**, 2437 (1977).
- [3] C. Kim, Z.X. Shen, N. Motoyama, H. Eisaki, S. Uchida, T. Tohyama and S. Maekawa, Phys. Rev. B **56**, 15589 (1997).
- [4] E. Lieb and F.Y. Wu, Phys. Rev. Lett. **20**, 1445 (1968).
- [5] H.J. Schultz, Int. J. Mod. Phys. B **5**, 57 (1991).
- [6] M. Brech, J. Voit and H. Büttner, Europhys. Lett. **12**, 289 (1990).
- [7] F.D.M. Haldane, J. Phys. C **14**, 2585 (1981)
- [8] J. Carmelo, P. Horsch, P.A. Bares and A.A. Ovchinnikov, Phys. Rev B**44**, 9967 (1991)
- [9] J. Riera, D. Poilblanc and E. Dagotto, Eur. Phys. J. B**7** 53 (1999).
- [10] M. Ogata and H. Shiba, Phys. Rev. B **41**, 2326 (1990).
- [11] N. Yu and M. Fowler Phys. Rev. B **45**, 11795 (1992).
- [12] Kusmartsev F.V., Phys. Rev. B **52**, 14445 (1995).
- [13] A.J. Schofield, J.M. Wheatley and T. Xiang, Phys. Rev. B**44**, 8349 (1991)
- [14] C. Kim, A.Y. Matsura, Z.X. Shen, N. Motoyama, H. Eisaki, S. Uchida, T. Tohyama and S. Maekawa, Phys. Rev. Lett. **77**, 4054 (1996).
- [15] R. Eder and Y. Ohta Phys. Rev. B **56**, 2542 (1997).
- [16] T. Tohyama and S. Maekawa J. Phys. Soc. Jpn. **65**, 1902 (1996).
- [17] E. Dagotto, Rev. Mod. Phys. **66**, 763 (1994).
- [18] K. Penc, K. Hallberg, F. Mila and H. Shiba, Phys. Rev. Lett. **77**, 1390 (1996).
- [19] S. Sorella and A. Parola, J. Phys.: Condens. Matter **4**, 3589 (1992).
- [20] J. Voit., Rep Prog. Phys. **58**, 977 (1995).
- [21] Preliminary studies on systems of coupled chains as function of the interchain coupling suggest that the spectral function shows evidence of spin-charge separation for non-zero interchain coupling, R.N. Bannister to be published. See also G.B. Martins, R. Eder and E. Dagotto, cond-mat/9904030.